Hindawi
Advances in Materials Science and Engineering
Volume 2018, Article ID 9861894, 9 pages
https://doi.org/10.1155/2018/9861894

Research Article

Synthesis of Ti_2SnC under Optimized Experimental Parameters of Pressureless Spark Plasma Sintering Assisted by Al Addition

Chen Lu, Yue Wang, Xiaofan Wang, and Jianfeng Zhang

College of Mechanics and Materials, Hohai University, Nanjing 210098, China

Correspondence should be addressed to Jianfeng Zhang; jfzhang_sic@163.com

Received 11 November 2017; Revised 19 January 2018; Accepted 18 February 2018; Published 27 March 2018

Academic Editor: Yee-wen Yen

As an effective and novel rapid sintering technology with the advantages of fast heating speed and short sintering time, SPS has been applied to the research and development of various materials. After sintering at 1325°C, Ti_5Sn_3 and Sn occurred as impurities accompanying the synthesis of Ti_2SnC with a raw powder mixture of Ti/Sn/C = 2/1/1 (molar ratio). But by addition of 0.2 molar Al, and further optimization of sintering parameters at 1400°C for 10 min, almost fully pure Ti_2SnC was obtained with a clear layered microstructure. The reaction mechanism analysis suggests that this beneficial effect of Al could be attributed to the suppression of decomposition of Ti_2SnC by formation of $Ti_2Sn_xAl_{1-x}C$ solid solution at a high sintering temperature. The present study reports a novel route to synthesize Ti_2SnC by PL-SPS with a self-designed graphite die, and Al was also proposed as a sintering aid to remove impurities.

1. Introduction

In the 1960s, the Nowotny team [1] pioneered the concept of ternary transition metal carbides or carbonitrides and discovered a variety of compounds with similar structures. Almost forty years later, Barsoum et al. classified these materials as $M_{n+1}AX_n$ phases(or MAX phases), wherein M is a transition metal element, A is a family of IIIA or IVA element, X is a C or N element, and n is generally 1, 2 or 3 [2–4]. Among these compounds, Ti_2SnC is one of the most attractive materials for its excellent properties of low hardness, eminent electrical conductivity, high modulus elasticity, high fracture toughness, self-lubrication, high chemical resistance, and good thermal stability [5–9]. Therefore, it is promising as a new generation of motor brush materials, heat exchanger materials, and various antifriction wear parts, chemical reactor mixer bearings, fan bearings, and special mechanical seals [6].

Up to now, Ti_2SnC has been synthesized by various methods mostly using the powder mixture of Ti/Sn/C elements or their compounds [10–14]. In consideration of large-scale fabrication possibility, self-propagating high-temperature synthesis (SHS), and pressureless sintering have been paid much attention due to their simplicity and easy operation [15]. However, unexpected impurities, such as TiC, Ti_6Sn_5, and or Sn, are usually found to accompany the formation of Ti_2SnC in these processes. Although some researchers have tried to increase the purity by tailoring the molar ratio of Ti–Sn–C or Ti–Sn–TiC, the almost complete conversion of the raw material to the desired ternary compound is still a big challenge [16].

Spark plasma sintering (SPS) has been emerging for more than thirty years as a modern method to produce advanced ceramics with great application prospects due to its rapid sintering rate and low sintering temperature [17–19]. Most recently, pressureless spark plasma sintering has been realized as a promising method for special requirements [20–22]. For example, Dudina et al. chose pressureless spark plasma sintering as the treatment method for reactive sintering of porous FeAl which reduces the time of high-temperature exposure thus short ending the sample shrinkage time [23]. By using this method, single-phase FeAl powders can be obtained at 800°C for the reason that electric current can be heated rapidly and uniformly distributed in the whole volume of the powder sample. Through coupling the combined aspect of conventional pressureless sintering with fast heating, Sairam et al. synthesized about 90% density of CrB_2 at 1900°C to 2000°C by multistep PL-SPS [24]. To the

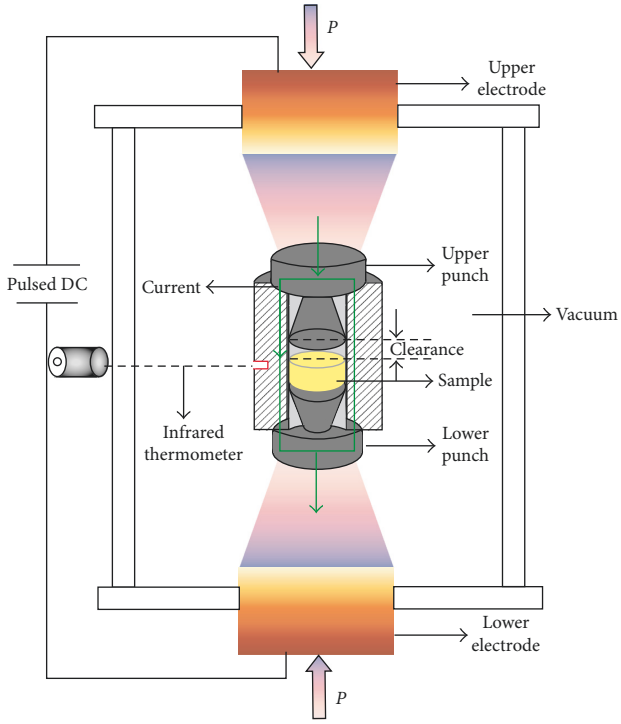

Figure 1: A schematic of SPS for synthesis without pressure.

best of our knowledge, however, the synthesis of MAX by PL-SPS has not been reported yet.

In this study, Ti_2SnC was synthesized from mixed powders of Ti/Sn/C using Al as a sintering aid by a PL-SPS process with a specially designed graphite die. Adding Al can prevent the generation of impurities in sintering MAX phases as reported [25]. The effects of molar ratio and other experimental parameters on the formation and morphology Ti_2SnC were investigated attentively. The reaction routes and mechanism were proposed through experimental and theoretical analysis.

2. Experimental Details

Powders of Ti (99.9% purity, 20 μm), Sn (99.9% purity, 3 μm), Al (99.9% purity, 40 μm), and C (99.9% purity, 15 μm) were mixed using an agate mortar in ethanol for 8 h with different molar ratios. Then, the mixed powders were precompacted in a drying cabinet and put into a self-designed graphite die with two fastigiated T-shape punches (10 mm front diameter and a 8 mm rear side die) for achieving the effect of pressureless sintering on both ends of the sleeve (50 mm in height, 10 mm in inner diameter, and 30 mm in outer diameter), which applied pressure on the punches instead of the powders (Figure 1). The specific sintering current and pressure are adopted to the die by using the upper and lower T-shape punches. It is known that by using Al and Sn with low melting points, the gas releasing and punch sticking to sleeve should be hindered to avoid the composition segregation. Combined with optimized sintering parameters, including temperature, holding time, and so on, such T-shape punches with fastigiated ends are best for demoulding to make the graphite dies reusable. A layer of carbon paper was wound on the graphite mold in order to avoid bonding between powders and graphite die in the sintering process [26]. Then, the graphite die was heated at 100°C/min in SPS furnace (SPS-2040 Japan) filled with Ar, at low temperature about 550°C, in order to promote the formation of Ti–Sn–Al intermetallics; 3 min residence time is in the process of binding. Then the graphite die was held at a target temperature from 800°C to 1500°C for 10 min. The as-synthesized samples were determined by X-ray diffraction (XRD, Bruker D8 Advance) to identify the phase composition, and the microstructure of the product sintered in the 800°C to 1500°C was characterized by field emission scanning electron microscopy (FE-SEM, S4800) equipped with an energy dispersive spectroscopy (EDS).

3. Results and Discussion

3.1. Effect of Molar Ratio on the Formation and Morphology of Ti_2SnC. Figure 2 shows the XRD patterns of products at the temperature 1325°C with different molar ratios of Ti : Sn : Al : C = (a) 2 : 1 : 0 : 1; (b) 2 : 1 : 0.05 : 1; (c) 2 : 1 : 0.1 : 1; (d) 2 : 1 : 0.15 : 1; (e) 2 : 1 : 0.2 : 1; (f) 2 : 1 : 0.3 : 1 in which the corresponding SEM images of the fracture surfaces were also embedded for reference. Firstly, it is clear to observe different phase compositions with the addition of Al. When adding Al, the new diffraction peak of Ti_2SnC is shown in Figure 2(b) such as β(006), β(105), and β(110). But no Al (Figure 2(a)) favors the formation of Ti_5Sn_3 and a few impurities. In Figure 2 however with increasing Al ratio to 0.2, the peak height of Ti_2SnC increased and a few Ti_3Al appears. The typical layered morphology at the Al ratio of 0.2

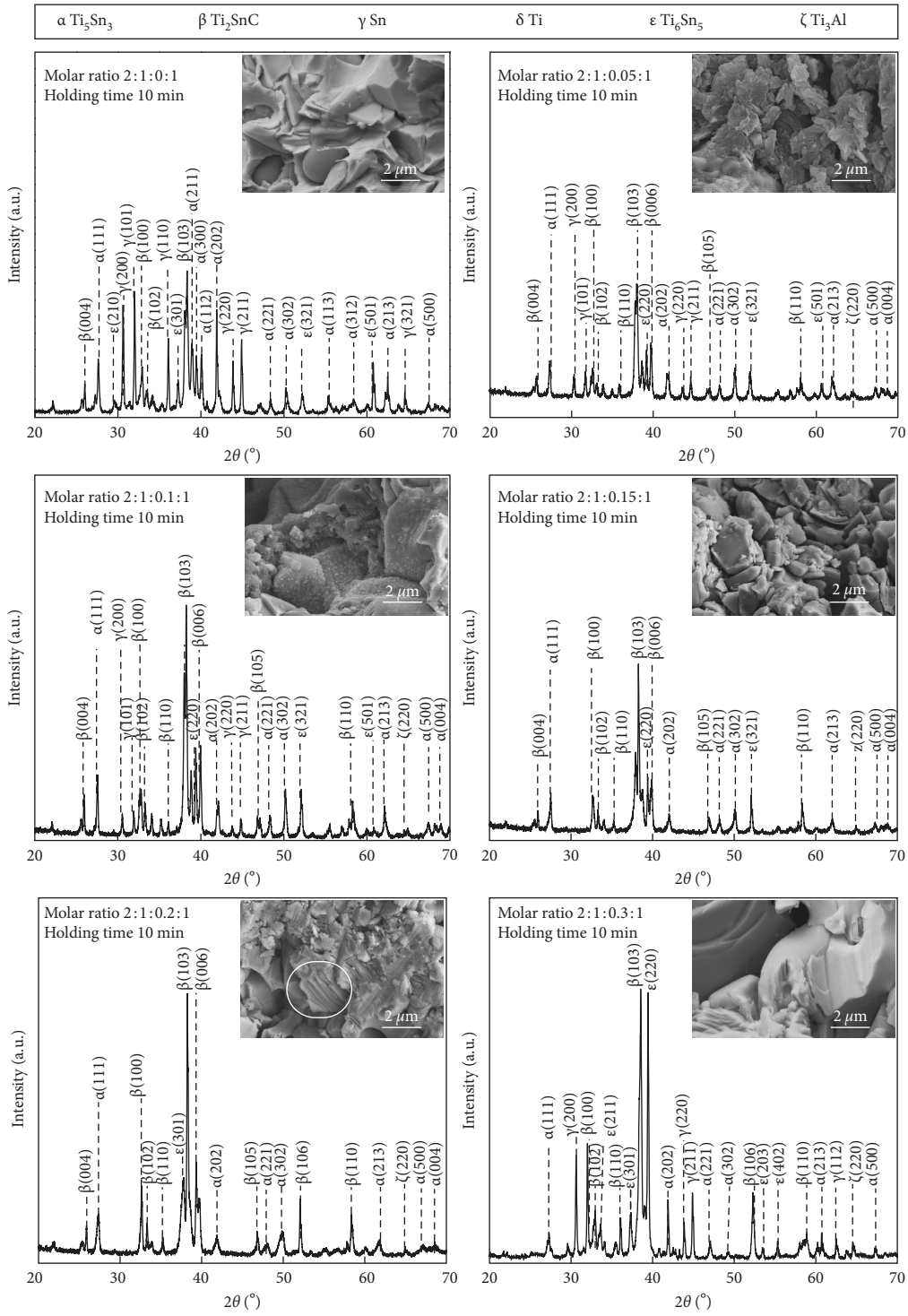

Figure 2: Sintering powders Ti_2SnC at different molar ratios Ti : Sn : Al : C = (a) 2 : 1 : 0 : 1; (b) 2 : 1 : 0.05 : 1; (c) 2 : 1 : 0.1 : 1; (d) 2 : 1 : 0.15 : 1; (e) 2 : 1 : 0.2 : 1; (f) 2 : 1 : 0.3 : 1 at 1325°C.

should also be mentioned here, validating our conjecture for the formation of Ti_2SnC. From Figure 3, the diffraction peak of Ti_2SnC (β(103)) shifts to a larger angle with an increase in Al from 0.05 to 0.2, indicating that the addition of Al could be reported to benefit the deletion of the impurities in Ti_2SnC since the solid solutions were produced.

3.2. Effect of Sintering Temperature and Holding Time on the Formation and Morphology of Ti_2SnC. Figure 4(a) shows the effects of (a) sintering temperature and (b) holding time on the peak ratio of Sn/Ti_2SnC and Ti_5Sn_3/Ti_2SnC at a molar ratio of 2 : 1 : 0.2 : 1 for Ti : Sn : Al : C. As shown in Figure 4(a), with increasing the sintering temperature from 1325°C to

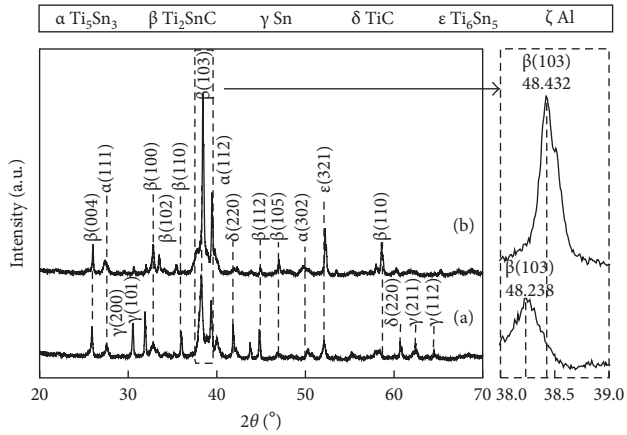

Figure 3: Sintering powders Ti_2SnC at different molar ratios Ti : Sn : Al : C = (a) 2 : 1 : 0.05 : 1; (b) 2 : 1 : 0.2 : 1 at 1400°C.

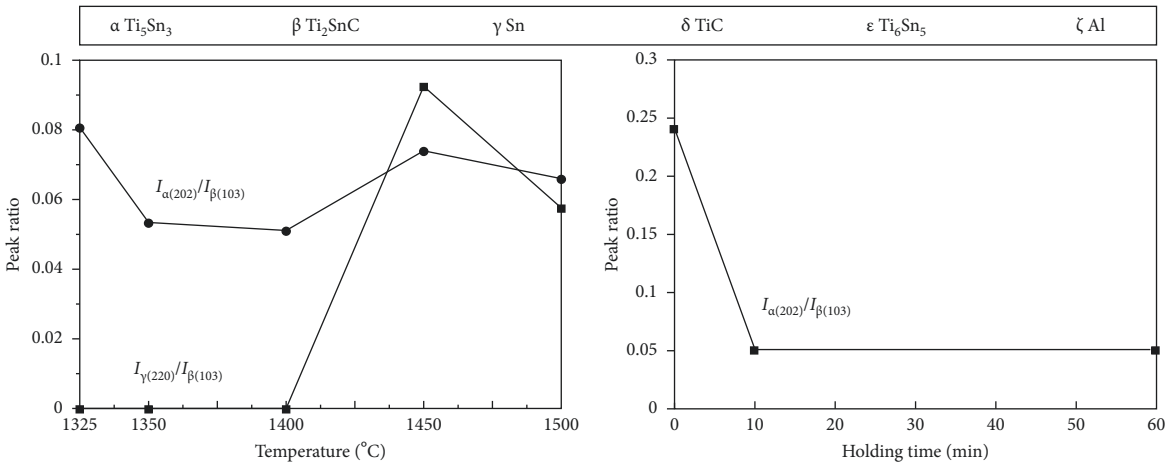

Figure 4: Effect of (a) sintering temperature holding time and (b) holding time on the peak ratio of Ti_5Sn_3/Ti_2SnC and Sn/Ti_2SnC at a molar ratio of 2 : 1 : 0.2 : 1 for Ti : Sn : Al : C.

1500°C, the peak intensity of $Ti_2SnC(I_{β(103)})$ increased, whereas the impurity of titanium tin compound (Ti_5Sn_3) decreased inversely, indicating that the purity of Ti_2SnC was elevated. With further increasing the sintering temperature to 1400°C, however, the peak ratio of both $I_{α(202)}/I_{β(103)}$ and $I_{γ(220)}/I_{β(103)}$ increased, suggesting that the impurity content of Ti_5Sn_3 and Sn unexpectedly decreased due to the decomposition of Ti_2SnC at a higher temperature, for which Sn was released to leave Ti_xSn_y dissociated [27, 28]. Moreover, the result peak ratio of $I_{α(202)}/I_{β(103)}$ is lower than the previous results, indicating that the impurity was decreased effectively [29]. But the effect of holding time is almost negligible since the purity kept almost the same after extending the holding time from 10 to 60 min at 1400°C (Figure 4(b)).

On the other hand, consolidation of Ti_2SnC at a pressure of 100 MPa from the same raw powder mixture of 2 : 1 : 0.2 : 1 for Ti : Sn : Al : C was also conducted for comparison with that by PL-SPS. As shown in Figure 5, before the sintering temperature increased near 1400°C (about 1370°C), the graphite die was found to be broken in the SPS furnace, which could be attributed to the release of liquid Sn impurity from the decomposition of Ti_2SnC, and the as-obtained sample was identified to be composed by Sn as well as Ti_6Sn_5 and TiC, inducing the extremely lower content of Ti_2SnC [30]. Such comparison validates PL-SPS as more competitive compared with SPS for synthesis of Ti_2SnC powders. Compared to conventional pressureless sintering for Ti_2SnC MAX phase, pressureless spark plasma sintering (PL-SPS) has the merits of short sintering time at almost 10 minutes and rapid temperature increasing/decreasing rate (100°C/min). By optimization of the experimental parameters, this method is quite available for fabrication of high purity MAX powders with a low cost and high efficiency.

3.3. Reaction Mechanism. Vincent et al. have studied the stability of Ti_2SnC in Al liquid and found that Ti_2SnC tended to be decomposed completely according to the following formula at a temperature above 1000°C [31]:

$$Ti_2SnC + 3Al(l) \rightarrow Al_3Ti + TiC + Sn \quad (1)$$

However, it should be noticed that the addition of minor Al also facilitates the formation of highly pure Ti_2SnC by PL-SPS in our present study, which is an interesting

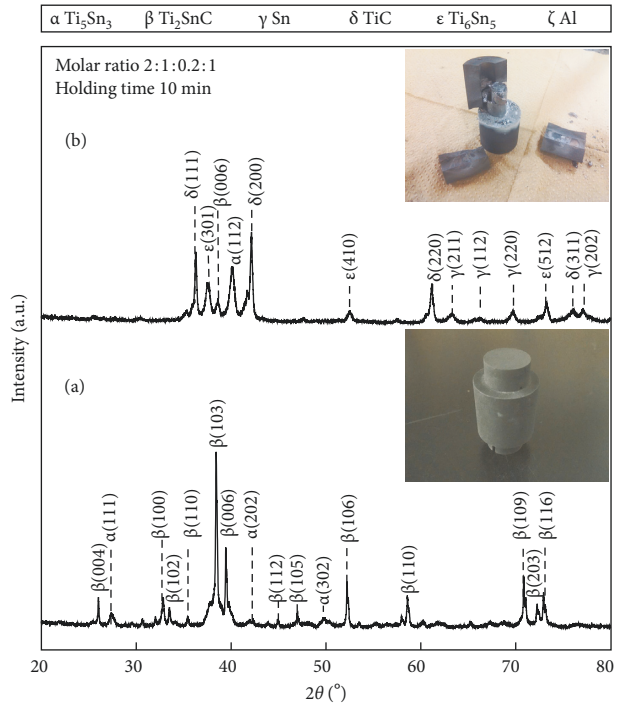

Figure 5: XRD pattern and SEM of the sample with molar ratio 2 : 1 : 0.2 : 1 at 1400°C sintering temperature on pressure of (a) 0 and (b)100 MPa.

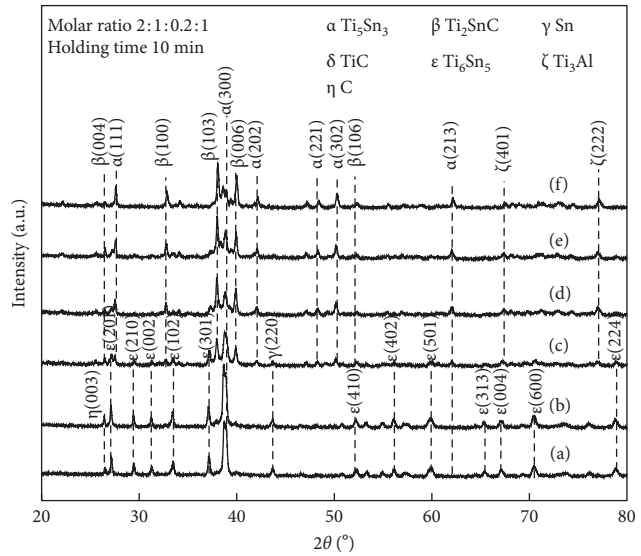

Figure 6: Sintering of sample Ti : Sn : Al : C = 2 : 1 : 0.2 : 1 of Ti_2SnC at (a) 800°C, (b) 900°C, (c) 1000°C, (d) 1100°C, (e) 1200°C, and (f) 1300°C on 10 minutes holding time.

phenomenon that needs explanation. The reason is that Al decreases the residual impurities, which will be elaborated as follows.

The optimized powder mixture of 2 : 1 : 0.2 : 1 for Ti : Sn : Al : C was sintered at 800°C to 1300°C to declare the formation mechanism by SPS, and the XRD patterns of as-obtained samples are shown in Figure 6. At 800°C, Ti_6Sn_5 appeared in XRD results and then decreased continuously with increasing temperature and turned to Ti_5Sn_3 at 1000°C due to the reaction with Ti. The XRD patterns of Ti_3Al also appear at about 1000°C. It is astonishing that the target product Ti_2SnC started to appear at a low temperature of 1000°C, accompanied by Ti_5Sn_3, Sn, and TiC. Figure 7 shows the TG-DSC-DTG curve of Ti_2SnC with ratio Ti : Sn : Al :

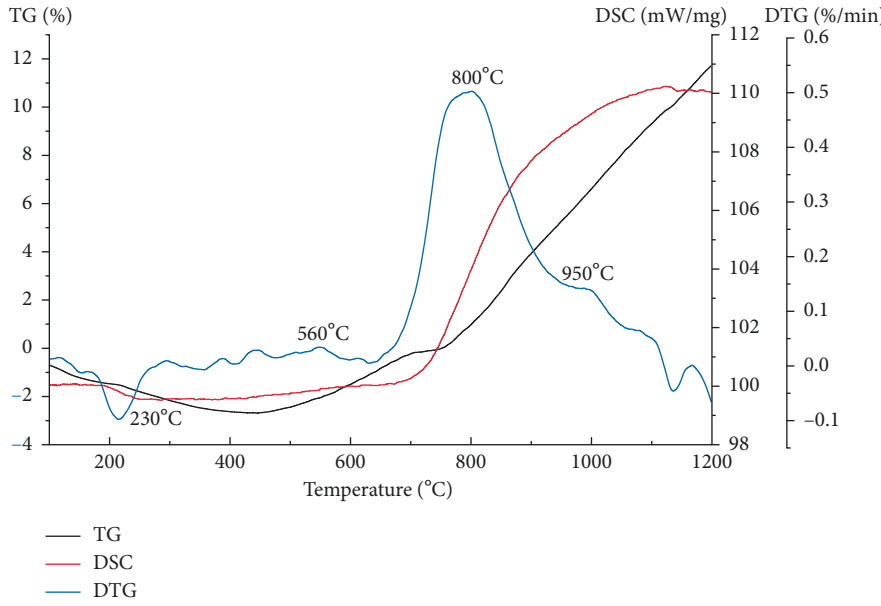

Figure 7: TG-DSC-DTG curve of Ti_2SnC with ratio Ti : Sn : Al : C = 2 : 1 : 0.2 : 1 at 1400°C.

C = 2 : 1 : 0.2 : 1 heated at a rate of 10°C/min from room temperature to 1200°C. The sharp endothermic peak at 230°C corresponds to the melting of Sn. The other exothermic peak was observed at 560°C, 800°C, and 950°C clarify the reaction route of the Ti/Sn/C system.

In consideration of the results by Li et al. [15] and the present work, and combined with the figure diagram (Figure 8) [32], the possible reaction routes are proposed as follows:

$$230^{\circ}C \quad Sn\,(s) \rightarrow Sn\,(l) \tag{2}$$

$$560^{\circ}C \quad Ti + Sn \rightarrow Ti_2Sn_3 \tag{3}$$

$$800^{\circ}C \quad Ti + Ti_2Sn_3 \rightarrow Ti_6Sn_5 \tag{4}$$

$$1000^{\circ}C \quad Ti_6Sn_5 + Ti \rightarrow Ti_5Sn_3 \tag{5}$$

$$Ti + C \rightarrow TiC \tag{6}$$

$$TiC + Ti_5Sn_3 \rightarrow Ti_2SnC \tag{7}$$

However, it should also be mentioned that Al could consume Ti by forming Ti–Al intermetallics [33]. In consideration of minor content of Al, the formation of Ti_mAl_n (Ti_3Al) should be taken into consideration for formation of $Ti_2Sn_xAl_{(1-x)}C$ solid solution.

$$660^{\circ}C \quad Al\,(s) \rightarrow Al\,(l) \tag{8}$$

$$950^{\circ}C \quad 3Ti + Al \rightarrow Ti_3Al \tag{9}$$

$$1000^{\circ}C\text{–}1400^{\circ}C \quad Ti_mAl_n + Ti_2SnC + TiC \rightarrow Ti_2Sn_xAl_{(1-x)}C \tag{10}$$

Figures 9 and 10 show the microstructures of the powders sintering at 800°C, 1000°C, and 1200°C. In Figure 9(c),

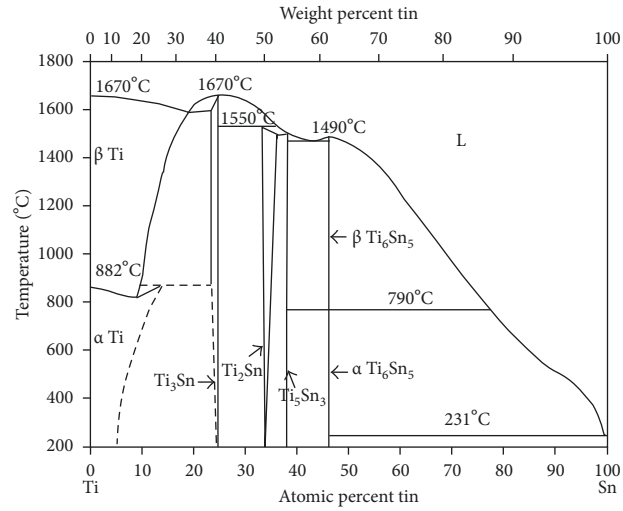

Figure 8: Phase diagram of Ti and Sn system (from Murray [30]).

layered structure starts to appear which is considered as Ti_2SnC validated by EDS spectrum. The layered structure with the size between 10 μm and 12 μm is more obvious at 1200°C. From Figures 6 and 9, the results suggest that the formation of Ti_2SnC is in accord with previous work [7, 9, 11, 14]. Therefore, the modified reaction route for the synthesis of Ti_2SnC assisted by Al can be clarified based on this consideration, as shown in Figure 11. By increasing the sintering temperature gradually, Sn and Al from the raw powder mixture start to melt successively. Then, intermetallics Ti_5Sn_3 starts to form as shown in Figure 11(b). When increasing the sintering temperature further, the impurity phase of TiC appears as validated combined with Ti_mAl_n (most possibly Ti_3Al) [34–36], and simultaneously, $Ti_2Sn_xAl_{1-x}C$ formed in Figure 11(c). As the sintering temperature goes near

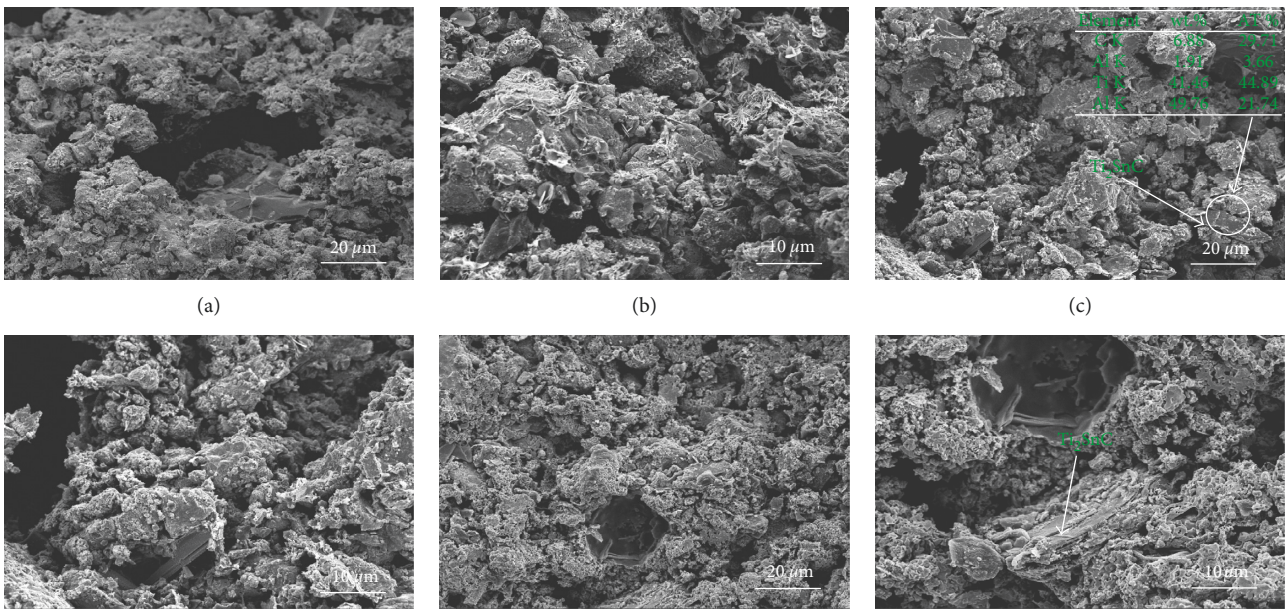

FIGURE 9: SEM and EDS micrographs of Ti_2SnC with ratio Ti : Sn : Al : C = 2 : 1 : 0.2 : 1 at (a and b) 800°C, (c and d) 1000°C, and (e and f) 1200°C.

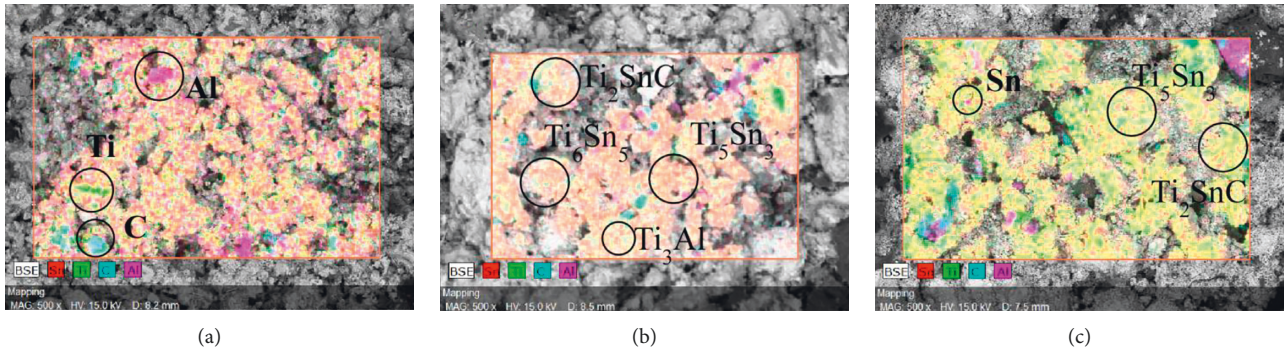

FIGURE 10: EDS micrographs of Ti_2SnC with ratio Ti : Sn : Al : C = 2 : 1 : 0.2 : 1 at (a) 800°C, (b) 1000°C, and (c) 1200°C.

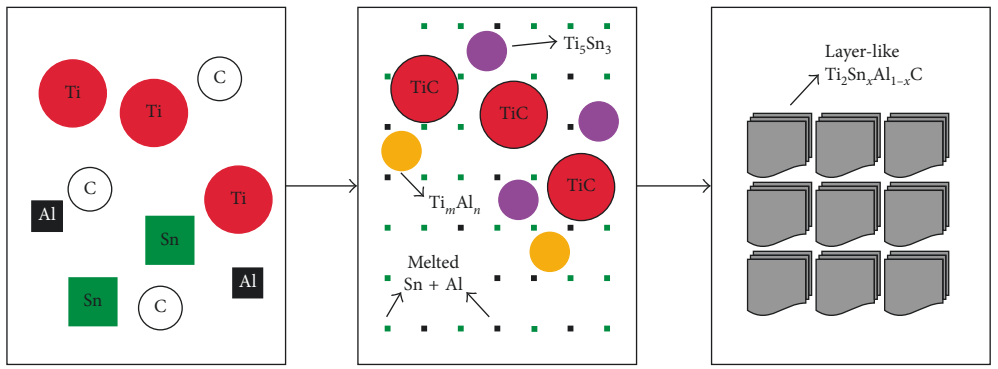

FIGURE 11: Schematic illustration of the route from mixing of elemental powders to the final interleaved layers of $Ti_2Sn_xAl_{1-x}C$. (a) Starting Ti/Sn/Al/C powders; (b) formation of TiC, Ti_5Sn_3 and Ti_mAl_n; (c) restraint of impurity and formation of layer $Ti_2Sn_xAl_{1-x}C$.

1400°C, almost fully pure $Ti_2Sn_xAl_{1-x}C$ formed by the whole reaction of TiC, Ti_mAl_n, and Ti_5Sn_3, and $Ti_2Sn_xAl_{1-x}C$ promotes the preparation of layer-like Ti_2SnC [14, 27].

4. Conclusions

Ti_2SnC was obtained by PL-SPS using Al as a sintering aid. The addition of Al was found to favor the fabrication Ti_2SnC by preventing the generation of Sn-like impurities and formation of $Ti_2Sn_xAl_{1-x}C$ solid solution at optimized sintering parameters of 1400°C for 10 min. But with further increasing the temperature, Sn impurity increased due to the incurable decomposition of Ti_2SnC. By PL-SPS, we prepared porous compact Ti_2SnC. The present study also validates PL-SPS as a promising method to synthesize MAX phase by careful experimental design and parameter optimization.

Conflicts of Interest

The authors declare that they have no conflicts of interest.

Acknowledgments

The authors would like to acknowledge the financial supports from Fundamental Research Funds for the Central Universities (2015B01914), the National Natural Science Foundation of China (51301059), the Natural Science Foundation of Jiangsu Province (BK20161506), the Opening Project of State Key Laboratory of Advanced Technology for Materials Synthesis and Processing (Wuhan University of Technology, 2016-KF-8), and the National 973 Plan Project (2015CB057803).

References

[1] V. H. Nowotny, "Strukturchemie einiger Verbindungen der Übergangsmetalle mit den elementen C, Si, Ge, Sn," *Progress in Solid State Chemistry*, vol. 5, pp. 27–70, 1971.

[2] M. W. Barsoum and T. Elraghy, "The MAX phases: unique new carbide and nitride materials," *American Scientist*, vol. 89, no. 4, pp. 334–343, 2001.

[3] Y. Medkour, A. Bouhemadou, and A. Roumili, "Structural and electronic properties of M_2InC (M = Ti, Zr, and Hf)," *Solid State Communications*, vol. 148, no. 9-10, pp. 459–463, 2008.

[4] A. Abdulkadhim, T. Takahashi, D. Music, F. Munnik, and J. M. Schneider, "MAX phase formation by intercalation upon annealing of TiC_x/Al ($0.4 \leq x \leq 1$) bilayer thin films," *Acta Materialia*, vol. 59, no. 15, pp. 6168–6175, 2011.

[5] M. W. Barsoum, "The $M_{N+1}AX_N$ phases: a new class of solids: thermodynamically stable nanolaminates," *Progress in Solid State Chemistry*, vol. 28, no. 1–4, pp. 201–281, 2000.

[6] J. Y. Wu, Y. C. Zhou, and J. Y. Wang, "Tribological behavior of Ti_2SnC particulate reinforced copper matrix composites," *Materials Science and Engineering: A*, vol. 422, no. 1-2, pp. 266–271, 2006.

[7] H. Y. Dong, C. K. Yan, S. Q. Chen, and Y. C. Zhou, "Solid–liquid reaction synthesis and thermal stability of Ti_2SnC powders," *Journal of Materials Chemistry*, vol. 11, no. 5, pp. 1402–1407, 2001.

[8] Y. Li and P. Bai, "The microstructural evolution of Ti_2SnC from Sn–Ti–C system by Self-propagating high-temperature synthesis (SHS)," *International Journal of Refractory Metals and Hard Materials*, vol. 29, no. 6, pp. 751–754, 2011.

[9] S. B. Li, G. P. Bei, H. X. Zhai, and Y. Zhou, "Bimodal microstructure and reaction mechanism of Ti_2SnC synthesized by a high-temperature reaction using Ti/Sn/C and Ti/Sn/TiC powder compacts," *Journal of the American Ceramic Society*, vol. 89, no. 12, pp. 3617–3623, 2006.

[10] S. B. Li, G. P. Bei, H. X. Zhai, Y. Zhou, and C. W. Li, "Synthesis of Ti_2SnC at low-temperature using mechanically activated sintering process," *Materials Science and Engineering: A*, vol. 457, no. 1-2, pp. 282–286, 2007.

[11] Y. Zhou, H. Dong, X. Wang, and C. Yan, "Preparation of Ti_2SnC by solid–liquid reaction synthesis and simultaneous densification method," *Materials Research Innovations*, vol. 6, no. 5-6, pp. 219–225, 2002.

[12] C. L. Yeh and C. W. Kuo, "Effects of TiC addition on formation of Ti_2SnC by self-propagating combustion of Ti–Sn–C–TiC powder compacts," *Journal of Alloys and Compounds*, vol. 502, no. 2, pp. 461–465, 2010.

[13] S. Li, L. Zhang, W. Yu, and Y. Zhou, "Precipitation induced crack healing in a Ti_2SnC ceramic in vacuum," *Ceramics International*, vol. 43, no. 9, pp. 6963–6966, 2017.

[14] S. B. Li, G. P. Bei, H. X. Zhai, and Y. Zhou, "Synthesis of Ti_2SnC from Ti/Sn/TiC powder mixtures by pressureless sintering technique," *Materials Letters*, vol. 60, no. 29-30, pp. 3530–3532, 2006.

[15] Y. Li, P. Bai, and B. Liu, "Effect of C/Ti ratio on self-propagating high-temperature synthesis reaction of Sn–Ti–C system for fabricating Ti_2SnC ternary compounds," *Journal of Alloys and Compounds*, vol. 509, no. 35, pp. L328–L330, 2011.

[16] H. Y. Sun, X. Kong, S. Wei, Z. Z. Yi, B. S. Wang, and G. Y. Liu, "Effects of different Sn contents on formation of Ti_2SnC by self-propagating high-temperature synthesis method in Ti-Sn-C and Ti-Sn-C-TiC systems," *Materials Science-Poland*, vol. 32, no. 4, pp. 696–701, 2014.

[17] J. Wang and G. Lian, "Photoluminescence properties of nanocrystalline ZnO ceramics prepared by pressureless sintering and spark plasma sintering," *Journal of the American Ceramic Society*, vol. 88, no. 6, pp. 1637–1639, 2005.

[18] S. H. Lee, H. Tanaka, and Y. Kagawa, "Spark plasma sintering and pressureless sintering of SiC using aluminum borocarbide additives," *Journal of the European Ceramic Society*, vol. 29, no. 10, pp. 2087–2095, 2009.

[19] M. Descamps, L. Boilet, G. Moreau et al., "Processing and properties of biphasic calcium phosphates bioceramics obtained by pressureless sintering and hot isostatic pressing," *Journal of the European Ceramic Society*, vol. 33, no. 7, pp. 1263–1270, 2013.

[20] D. Zheng, X. Li, Y. Tang, and T. Cao, "WC–Si_3N_4 composites prepared by two-step spark plasma sintering," *International Journal of Refractory Metals and Hard Materials*, vol. 50, pp. 133–139, 2015.

[21] B. Yavas and G. Goller, "Investigation the effect of B_4C addition on properties of TZM alloy prepared by spark plasma sintering," *International Journal of Refractory Metals and Hard Materials*, vol. 58, pp. 182–188, 2016.

[22] M. B. Shongwe, S. Diouf, M. O. Durowoju, P. A. Olubambi, M. M. Ramakokovhu, and B. A. Obadele, "A comparative study of spark plasma sintering and hybrid spark plasma sintering of 93W–4.9Ni–2.1Fe heavy alloy," *International Journal of Refractory Metals and Hard Materials*, vol. 55, pp. 16–23, 2016.

[23] D. V. Dudina, M. A. Legan, N. V. Fedorova, A. N. Novoselov, A. G. Anisimov, and M. A. Esikov, "Structural and mechanical

characterization of porous iron aluminide FeAl obtained by pressureless spark plasma sintering," *Materials Science and Engineering: A*, vol. 695, pp. 309–314, 2017.

[24] K. Sairam, J. K. Sonber, T. S. R. C. Murthy, A. K. Sahu, R. D. Bedse, and J. K. Chakravartty, "Pressureless sintering of chromium diboride using spark plasma sintering facility," *International Journal of Refractory Metals and Hard Materials*, vol. 58, pp. 165–171, 2016.

[25] G. Bei, B. J. Pedimonte, T. Fey, and P. Greil, "Oxidation behavior of MAX phase $Ti_2Al_{(1-x)}Sn_xC$ solid solution," *Journal of the American Ceramic Society*, vol. 96, no. 5, pp. 1359–1362, 2013.

[26] K. Vanmeensel, A. Laptev, J. Hennicke, J. Vleugels, and O. Van der Biest, "Modelling of the temperature distribution during field assisted sintering," *Acta Materialia*, vol. 53, no. 16, pp. 4379–4388, 2005.

[27] J. Ding, P. Zhang, W. Tian et al., "The effects of Sn content on the microstructure and the formation mechanism of Ti_2SnC powder by pressureless synthesis," *Journal of Alloys and Compounds*, vol. 695, pp. 2850–2856, 2017.

[28] S. Li, G. Bei, X. Chen et al., "Crack healing induced electrical and mechanical properties recovery in a Ti_2SnC ceramic," *Journal of the European Ceramic Society*, vol. 36, no. 1, pp. 25–32, 2016.

[29] T. Lapauw, K. Vanmeensel, K. Lambrinou, and J. Vleugels, "Rapid synthesis and elastic properties of fine-grained Ti_2SnC produced by spark plasma sintering," *Journal of Alloys and Compounds*, vol. 631, pp. 72–76, 2015.

[30] J. L. Murray, *Phase Diagrams of Binary Titanium Alloys*, ASM International, Novelty, OH, USA, 1987.

[31] H. Vincent, C. Vincent, B. F. Mentzen, S. Pastor, and J. Bouix, "Chemical interaction between carbon and titanium dissolved in liquid tin: crystal structure and reactivity of Ti_2SnC with Al," *Materials Science and Engineering: A*, vol. 256, no. 1-2, pp. 83–91, 1998.

[32] G. P. Vassilev, E. S. Dobrev, and J. C. Tedenac, "Phase diagram of the Sn–Zn–Ti system," *Journal of Alloys and Compounds*, vol. 407, no. 1-2, pp. 170–175, 2006.

[33] Y. Sun, S. K. Vajpai, K. Ameyama, and C. Ma, "Fabrication of multilayered Ti–Al intermetallics by spark plasma sintering," *Journal of Alloys and Compounds*, vol. 585, pp. 734–740, 2014.

[34] B. Mei, W. Zhou, J. Zhu, and X. Hong, "Synthesis of high-purity Ti_2AlC by spark plasma sintering (SPS) of the elemental powders," *Journal of Materials Science*, vol. 39, no. 4, pp. 1471-1472, 2004.

[35] W. Jiang, L. Shi, L. Wang, and J. Zhang, "In situ fabrication of $TiC/Ti_3Al/Ti_2AlC$ composite by spark plasma sintering technology," *Journal of the Ceramic Society of Japan*, vol. 118, no. 1382, pp. 872–875, 2010.

[36] Y. L. Yue and H. T. Wu, "Fabrication of $Ti_2AlC/TiAl$ composites with the addition of niobium by spark plasma sintering," *Key Engineering Materials*, vol. 368–372, pp. 1004–1006, 2008.